

31% EUROPEAN INGAP/GAAS/INGANAS SOLAR CELLS FOR SPACE APPLICATION

Roberta Campesato¹ Antti Tukiainen², Arto Aho², Gabriele Gori¹, Riku Isoaho², Erminio Greco¹, Mircea Guina²

⁽¹⁾ CESI S.p.A., Via Rubattino 54, 20134 Milan, Italy: mail: campesato@cesi.it

⁽²⁾ Tampere University of Technology, Optoelectronics Research Centre, PO Box 692, FI-33101 Tampere, Finland

ABSTRACT

We report a triple junction InGaP/GaAs/InGaAs solar cell with efficiency of ~31% at AM0, 25 °C fabricated using a combined molecular beam epitaxy (MBE) and metal-organic chemical vapour deposition (MOCVD) processes. The prototype cells comprise of InGaAs (Indium Gallium Nitride Arsenide) bottom junction grown on a GaAs (Gallium Arsenide) substrate by MBE and middle and top junctions deposited by MOCVD. Repeatable cell characteristics and uniform efficiency pattern over 4-inch wafers were obtained. Combining the advantages offered by MBE and MOCVD opens a new perspective for fabrication of high-efficiency space tandem solar cells with three or more junctions. Results of radiation resistance of the sub-cells are also presented and critically evaluated to achieve high efficiency in EOL conditions.

1. INTRODUCTION

Space applications require more and more efficient solar cells. From the standard InGaP/InGaAs/Ge triple junction solar cells with AM0 efficiency >29%, research is addressing the development of more than three junction devices and the substitution of germanium with 1 eV materials in order to overcome 31% efficient solar cells. The highest efficiency, i.e. 35.8% at AM0, has been demonstrated for a 5-junction cell fabricated by direct semiconductor bonding technique, i.e. not a monolithic process [1]. Using MBE, monolithic lattice-matched solar cells with efficiencies as high as 44% measured in concentrated sunlight have been demonstrated [2]. The increase in efficiency compared to standard approaches is made possible owing to MBE's capability to synthesize high-quality dilute nitride alloys, such as InGaAsSb, which can be grown lattice matched onto GaAs or Ge substrates and exhibit a bandgap ranging from 0.8 eV to 1.43 eV. InGaAsSb can also be grown by MOCVD but the efficiency increase has been hindered by incorporation of impurities and high background carrier concentrations that are specific to MOCVD processes [3]. In contrast, using MBE, low background carrier concentrations and high quantum efficiency and current production have been demonstrated with high open-circuit voltage (V_{oc}) by MBE-grown 1 eV materials [4]. Even though MBE has proven to be compatible with mass production of III-V semiconductor devices, its use for volume

fabrication of solar cells has not yet been widely adopted, allegedly due to higher throughput offered by MOCVD.

In this paper, we report results obtained from III-V solar high-efficiency multi-junction solar cells grown by the MOCVD and MBE techniques. The technique presented in [5] combines two active solar cell junctions grown by different methods into single monolithic multi-junction structure. This opens a new perspective for fabrication of space tandem solar cells with three or more junctions.

2. THEORETICAL MODEL

The elevated complexity of a III-V multi-junction solar cell, in terms of number of layers, opto-electronic material properties and physical phenomena involved, makes a pure experimental optimization of the device impracticable. A reliable model is therefore necessary to boost the optimization process.

CESI developed a proprietary code to simulate the optical and the electrical behaviour of a multi-junction solar cell.

As concern the electrical model, each sub-cell is separately simulated taking into account the diffusion and the recombination dark currents relative to each junction according to a two diode model (Hovel).

Once the current voltage ($I-V$) curve of each sub-cell is determined, the $I-V$ curve of the multi-junction device is numerically calculated as the series of the n sub-cells that constitute the device. The effect of series and shunt resistances are also included in the model.

All of the electrical parameters of each semiconductor material used in the cell structure and necessary for the calculations (e.g. carrier mobility, electron and hole lifetimes, surface recombination velocity at interfaces etc.) are loaded in the material database. The database is continuously updated both from literature and from experimental results performed by CESI.

Of particular importance for a reliable simulation result are the optical interference effects not negligible for a structure where the thickness of the layers is comparable with the optical wavelengths.

The optical model implemented in CESI code is based on the transfer matrix formalism where each layer of the device is described by a 2×2 matrix and the stack of layers can then be represented by a matrix which is the product of the individual layer matrices [6]. This method allows calculation of the reflectivity and the

incident optical spectrum on each sub-cell taking into account the interference effects. As the electrical parameters of each material, the optical ones (refractive index and extinction coefficient) are entered in the material database.

The best methodology in order to optimize the device performances is an iterative approach: the solar cell structure is designed, simulated, manufactured and tested. The experimental results obtained from different characterization techniques (e.g. Spectral response, reflectivity, photoluminescence, current-voltage curve, Hall measurements etc.) provide the feedback needed to improve the input parameters to the code and then to restart the optimization.

The CESI model, updated for the optimization of a Triple junction InGaP/ GaAs/ InGaNAs solar cells, has been very useful in determination of the optimal band gaps and the thickness of the bases of the two top junctions (InGaP/GaAs).

The optimization of a solar cell manufactured using a combination of molecular beam epitaxy (MBE) and metal-organic chemical vapor deposition (MOCVD) processes is very challenging because it is also necessary to consider the effect of MOCVD overgrowth on the InGaNAs sub-cell. A typical effect due to MOCVD overgrowth is the shift of the external quantum efficiency (EQE) of dilute nitride junction towards shorter wavelengths. This effect is rather typical for dilute nitride heterostructures experiencing thermal annealing.

Therefore, the blue-shift of the band edge in InGaNAs must be included in the model in order to properly balance the photocurrent generated in each sub-cell and thus to optimize the device efficiency.

Using the code a theoretical efficiency of 32% is obtained for InGaP/InGaAs/InGaNAs solar cells at AM0, 25 C.

3. MANUFACTURING

The process for production of TJ solar cells using combined MBE-MOCVD technique consists in:

- Growth of InGaNAs junction on GaAs substrate by MBE;
- Transfer of wafers from MBE reactor to MOCVD reactor;
- Growth of GaAs and InGaP junction by MOCVD.

The InGaNAs junction was grown using a Veeco GEN20 MBE system. The MBE process was started by thermal desorption of the native oxides from an epi-ready 4" p-GaAs(100) substrate. A p-GaAs buffer layer followed by a lattice-matched p-InGaP back surface field layer were then grown. The p-i-n diode, consisting of a p-GaAs base layer, a nominally undoped InGaNAs layer and an n-GaAs emitter was grown next. The structure was finalized by growing window and contact layers that were used as transfer interface for the

MOCVD process. Additional details of the epitaxy of the InGaNAs sub-cells can be found elsewhere [4],[6–7].

After the MBE growth the substrates were transferred to the MOCVD system using a packaging procedure properly defined to reduce the possibility for contamination of the overgrowth interface.

InGaP and GaAs junctions were grown using a VEECO E450 MOCVD reactor. The nucleation layer was optimized to maintain a high quality interface between the MBE grown structure and MOCVD grown structure. An (Al)GaAs-based p^{++}/n^{++} tunnel junction was deposited after the nucleation layer. Then, the GaAs middle junction, the top tunnel junction and the InGaP top junction were deposited. The GaAs middle junction and the InGaP top junction had to be made thinner than those of the standard CESI InGaP/GaInAs/Ge (CTJ30) solar cell structure [8]. To determine the proper thickness for the GaAs junction, single n-GaAs overlayers with different thicknesses and thus with different growth and annealing times were deposited by MOCVD. Based on the effect of the thickness of the n-GaAs overlayer on the J_{sc} of the InGaNAs junction, the triple-junction solar cell structures were designed and fabricated using the combined MBE-MOCVD process.

The wafers were characterized using light microscopy (Leica DFC280 and Nikon L200) and PL (Accent RPM2000). Electrical characteristics of 2×2 cm² triple-junction solar cells were measured by $I-V$ and EQE. EQEs were measured using a self-made system comprising of a 250 W QTH lamp, a DK480 monochromator, a chopper, an infinity-corrected 50× Olympus objective lens, a NIST-calibrated Ge detector as a reference, electrical and optical biasing circuits for multi-junction cells, and a lock-in amplifier. $I-V$ measurements were taken using a dual source WACOM simulator that was calibrated at AM0 illumination using a Secondary Working Standard (SWS) set for the InGaP/GaAs/Ge triple-junction cell calibrated at Spasolab.

4. EXPERIMENTAL RESULTS

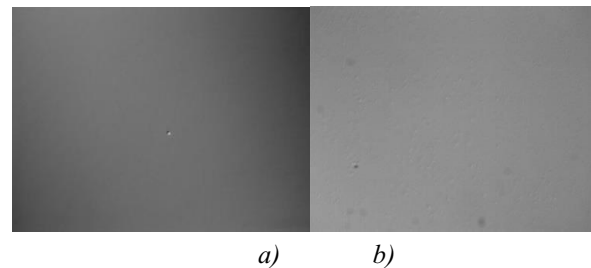


Figure 1. Surface micrographs taken from epiwafers a) with single-junction dilute nitride solar cell before MOCVD-regrowth
b) with triple-junction solar cell after the MOCVD process

Morphology of MBE-grown dilute nitride junctions showed only few surface defects. Mainly small defects with circular shape and typical oval defects (Fig. 1a) were detected. The number of surface defects, mainly conical ones, was slightly increased after MOCVD growth but the surface morphology was of high quality (Fig. 1b).

The behaviour of the short-circuit current density (J_{sc}) of the InGaNaS junction as a function of the thickness of the MOCVD-grown n-GaAs over layer is shown in Fig. 2. When the n-GaAs layer thickness is larger than $2\mu\text{m}$, the short circuit current of the dilute nitride junction falls below 18 mA/cm^2 .

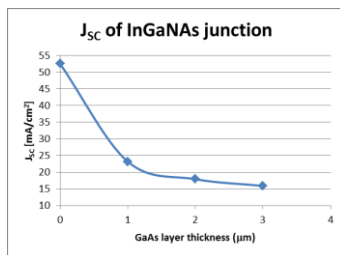


Figure 2. J_{sc} of the InGaNaS junction as a function of the thickness of the MOCVD-grown n-GaAs overlayer

The J_{sc} decrease after MOCVD growth is linked to the light absorption of the over layers and to the properties of dilute nitride junction that are altered by the annealing suffered during re-growth process as discussed in [5].

In fact, the energy gap of InGaNaS slightly increases as demonstrated by Photoluminescence and Spectral Response measurement reported in figure 3. As reported in [5] during the MOCVD process the emission peak corresponding to the dilute nitride junction is slightly shifted towards shorter wavelengths and this explains at least in part the reduced J_{sc} . Such behavior is rather typical for dilute nitride heterostructures experiencing thermal annealing [9–13].

The EQEs of dilute nitride junction before and after MOCVD overgrowth are shown in Fig. 3. Here the blueshift of the long wavelength edge of the EQE curve is visible as well and is related to blueshift of the band edge. The EQE is also increased due to MOCVD overgrowth for the shorter wavelengths.

As the MOCVD processes are typically run at higher temperature than the corresponding MBE processes and contain contaminants like hydrogen and carbon, it was expected that the MOCVD overgrowth could have an adverse effect on the properties of the InGaNaS junction either by thermal load or by introduction of impurities. Nevertheless, PL and EQE results indicate that the characteristics of the dilute nitride sub-cell were not degraded during overgrowth except for a slight blue shift of the absorption edge. An additional sign of preserving the high quality of dilute-nitride material was that the PL peak width did not get wider after

overgrowth.

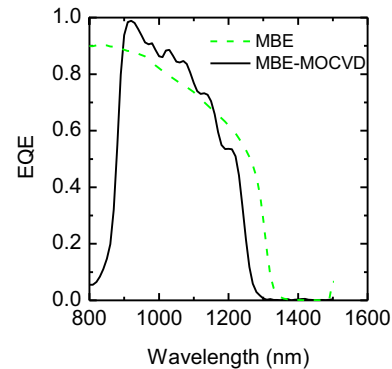


Figure 3. EQE measurements for a typical dilute nitride single-junction solar cell before the MOCVD process (solid black line) and for a dilute nitride sub-cell in a triple-junction solar cell after the MOCVD overgrowth process (dashed green line)

GaAs and InGaP junction were designed and their growth parameters optimized to produce TJ solar cells by the combined MBE-MOCVD technique. Design and optimization was made keeping into account the effects of MOCVD growth on the properties of the InGaNaS junction and improving the InGaP growth parameters. After the optimization, $2\times 2\text{ cm}^2$ solar cells with 30.8% AM0 efficiency at Beginning-Of-Life (BOL) were produced (Fig. 4).

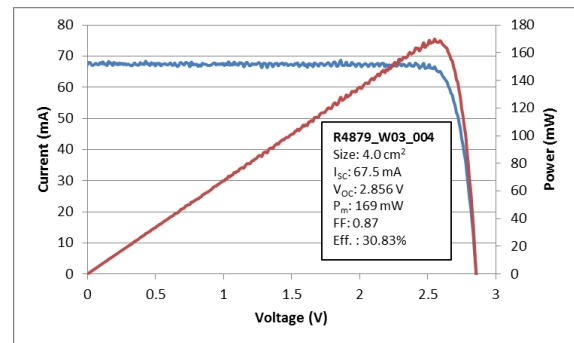


Figure 4. Electrical performances of InGaP/GaAs/InGaNaS triple-junction solar cells measured under dual source WACOM solar simulator at 1 sun, 25 °C

The main difference between experimental and theoretical expectation was related to the short circuit current (I_{sc}), mainly linked to InGaP junction that needs further improvements.

For optimization of End-Of-Life (EOL) efficiency of TJ solar cells, electron irradiation was performed on InGaP, GaAs and InGaNaS isotype solar cells. $2\times 2\text{ cm}^2$ solar cells were irradiated with 1 MeV electrons at $2E15\text{ e}^-/\text{cm}^2$ and $5E15\text{ e}^-/\text{cm}^2$ fluences. The irradiation was

executed at ILU-6 accelerator at Centre for Radiation Research and Technology of Institute of Nuclear Chemistry and Technology (INCT) in Warsaw (Poland). Remaining factors of isotype solar cells after irradiation are reported in Tab. 1 and Tab. 2.

Table 1: Remaining factors at $2E15\text{ e}^-/\text{cm}^2$ fluence

Solar cell structure	I_{sc} RF	V_{oc} RF	P_m RF
InGaP	0.99	0.97	0.95
GaAs	0.85	0.89	0.74
InGaNaS	0.69	0.90	0.59

Table 2: Remaining factors at $5E15\text{ e}^-/\text{cm}^2$ fluence

Solar cell structure	I_{sc} RF	V_{oc} RF	P_m RF
InGaP	0.97	0.95	0.89
GaAs	0.74	0.86	0.61
InGaNaS	0.56	0.82	0.40

The analysis of the short circuit currents of the three junctions to determine the limiting sub-cell and the EOL behaviour (table 3) is very intriguing: at BOL the limiting junction is the top one whereas after irradiation of $2e15\text{ e}^-/\text{cm}^2$, the limiting sub-cell is the middle.

Table 3: Short circuit currents of sub-cells after 1 MeV electrons (cell area $2\times 2\text{ cm}^2$)

I_{sc} (mA)	BOL	$2e15\text{ e}^-/\text{cm}^2$	$5e15\text{ e}^-/\text{cm}^2$
InGaP	68	66	65
GaAs	70	59	52
InGaNaS	98	72	52

To improve the EOL efficiency it is important to increase the current of the GaAs sub-cell. Following the model explained in chapter 3, the structure of the GaAs junction will be properly modified to increase its short circuit current without penalising the thermal load on the InGaNaS.

5. CONCLUSIONS

InGaP/GaAs/InGaNaS solar cells have been manufactured by a monolithic approach using the combination of MBE and MOCVD techniques.

The results indicate that efficiency near 31% in AM0, 25 °C is reachable. Comparison between the theoretical and experimental results also suggests that further improvement in the BOL efficiency can be obtained by optimization of the InGaP sub-cell.

EOL performance of the InGaP/GaAs/ InGaNaS solar cells is dominated by the behaviour of the middle junction. Therefore, to increase the EOL performance of the TJ solar cells the short circuit current of the GaAs sub-cell needs to be increased.

6. Acknowledgements

This work was performed under a programme of and funded by the European Space Agency (contracts N.: 4000108058/13/NL/FE, 4000112560/14/NL/FE). The view expressed herein can in no way be taken to reflect the official opinion of the European Space Agency.

7. REFERENCES

1. Chiu P. T., Law D. C., Woo R.L., Singer S. B., Bhusari D., Hong W. D., Zakaria A., Boisvert J., Mesropian S., King R. R., Karam N. H., Proceedings of the 40th IEEE PVSC, 2014, DOI: 10.1109/PVSC.2014.6924957.
2. Green M. A., Emery K., Hishikawa Y., Warta W., Dunlop E. D., Solar cell efficiency tables (version 41), Progress in Photovoltaics: Research and Applications 2013; 21: 1, DOI: 10.1002/pip.2352
3. Friedman D. J., Geisz J. F., Kurtz S. R., Olson J. M., 1-eV solar cells with GaInNaS active layer, Journal of Crystal Growth 1998; 195: 409, DOI: 10.1016/S0022-0248(98)00561-2.
4. Aho A., Tukiainen A., Polojärvi V., Korpjärvi V.-M., Gubanov A., Salmi J., Guina M., Laukkanen P., Lattice Matched Dilute Nitride Materials for III-V High-Efficiency Multi-Junction Solar Cells: Growth Parameter Optimization in Molecular Beam Epitaxy, Proceedings of the 26th EU PVSEC, 2011, 58, DOI:10.4229/26thEUPVSEC2011-1AO.8.3.
5. A. Tukiainen, A. Aho, G. Gori, V. Polojärvi, M. Casale, E. Greco, R. Isoaho, T. Aho, M. Raappana, R. Campesato and M. Guina, High-efficiency GaInP/GaAs/GaInNaS solar cells grown by combined MBE-MOCVD technique, Progress in Photovoltaics: Research and Applications, Accepted for publication, 2016.
6. Aho A., Tukiainen A., Korpjärvi V.-M., Polojärvi V., Salmi J., Guina M., Comparison of GaInNaS and InGaNaSb solar cells grown by plasma-assisted molecular beam epitaxy, AIP Conference Proceedings 2012: 49, DOI:10.1063/1.4753831.
7. Aho A., Polojärvi V., Korpjärvi V.-M., Salmi J., Tukiainen A., Laukkanen P., Guina M., Composition dependent growth dynamics in molecular beam epitaxy of GaInNaS solar cells, Solar Energy Materials and Solar Cells. 2014; 124: 150, DOI: 10.1016/j.solmat.2014.01.044.
8. Gori G., Campesato R.: Photovoltaic Cell Having a high Conversion Efficiency, PCT I09111-WO 2009

9. Klar P. J., Grüning H., Koch J., Schäfer S., Volz K., Stoltz W., Heimbrod W., (Ga, In)(N, As)-fine structure of the band gap due to nearest-neighbor configurations of the isovalent nitrogen, *Physical Review B* 2001; 64: 121203, DOI: 10.1103/PhysRevB.64.121203.
10. Pavelescu E.-M., Jouhti T., Dumitrescu M., Klar P.J., Karirinne S., Fedorenko Y., Pessa M., Growth-temperature-dependent (self-)annealing-induced blueshift of photoluminescence from 1.3 μm GaInNAs/GaAs quantum wells, *Applied Physics Letters* 2003; 83: 1497, DOI: 10.1063/1.1601309.
11. Kudrawiec R., Pavelescu E.-M., Andrzejewski J., Misiewicz J., Gheorghiu A., Jouhti T., Pessa M., The energy-fine structure of GaInNAs/GaAs multiple quantum wells grown at different temperatures and postgrown annealed, *Journal of Applied Physics* 2004; 96: 2909, DOI: 10.1063/1.1774258.
12. Karirinne S., Pavelescu E.-M., Konttinen J., Jouhti T., Pessa M., The behaviour of optical and structural properties of GaInNAs/GaAs quantum wells upon annealing, *New Journal of Physics* 2004; 6: 192, DOI: 10.1088/1367-2630/6/1/192.
13. Pavelescu E.-M., Wagner J., Komsa H.-P., Rantala T.T., Dumitrescu M., Pessa M., Nitrogen incorporation into GaInNAs lattice-matched to GaAs: The effects of growth temperature and thermal annealing, *Journal of Applied Physics*